

Dynamic Mechanical and Thermal Properties of PE-EPDM Based Jute Fiber Composites

Gautam Sarkhel, Arup Choudhury

Department of Polymer Engineering, Birla Institute of Technology, Mesra, Ranchi 835215, India

Received 7 February 2007; accepted 23 November 2007

DOI 10.1002/app.28024

Published online 6 March 2008 in Wiley InterScience (www.interscience.wiley.com).

ABSTRACT: The present investigation deals with the mechanical, thermal and viscoelastic properties of ternary composites based on low density polyethylene (LDPE)-ethylene-propylene-diene terpolymer (EPDM) blend and high density polyethylene (HDPE)-EPDM blend reinforced with short jute fibers. For all the untreated and compatibilizer treated composites, the variation of mechanical and viscoelastic properties as a function of fiber loading (10, 20 and 30 wt %) and compatibilizer concentration (1, 2, and 3%) were evaluated. The flexural strength, flexural modulus, impact strength, and hardness increased with increasing both the fiber loading and the compatibilizer dose. The storage modulus (E') and loss modulus (E'') of the HDPE-EPDM/jute fiber composites were recorded higher compared to those of the LDPE-EPDM/jute fiber composites at

all level of fiber loading and compatibilizer doses. The $\tan \delta$ (damping efficiency) spectra showed a strong influence of the fiber loading and compatibilizer dose on the α relaxation process of polymer matrix in the composite. The thermo-oxidative stability was significantly enhanced for treated composites compared to untreated composites. Scanning electron microscopy investigation confirmed that the higher values of mechanical and viscoelastic properties of the treated composites compared to untreated composites is caused by improvement of fiber-matrix adhesion as result of compatibilizer treatment. © 2008 Wiley Periodicals, Inc. *J Appl Polym Sci* 108: 3442–3453, 2008

Key words: composites; PE-EPDM blend; jute fibers; MAPE; mechanical and thermal properties; DMA; morphology

INTRODUCTION

Fiber reinforced thermoplastic composites are now finding suitable materials for various applications in automobile, building, electrical, and packaging sectors,^{1,2} because of their several practical advantages like ease of processing, fast production cycling, and low processing cost over traditional materials. In practice, these composite materials are designed to perform in different static and dynamic conditions.³ However, the interfacial bond strength between the reinforcing fibers and the resin matrix is an important aspect in achieving high performance of these composites.⁴ Nowadays, the natural fiber reinforced composites have received much attention in producing potential structural materials. The natural fibers (jute, sisal, coir, banana, and hemp) have many attractive characteristics like low density, less abrasiveness, low cost, biodegradability, and renewability over traditional glass and organic fibers (aramid and carbon fibers).^{5,6} However, the major drawback of the natural fiber-polymer composites is the inherent incompatibility between the hydrophilic fibers and the hydrophobic polymer matrix, which calls for improving the fiber-matrix interfacial adhesion by

using compatibilizers or coupling agents.^{7–9} Among the several natural fibers, jute constitutes a major area of investigation, because it is annually regenerative and lignocellulosic biopolymer based fiber.¹⁰

Dynamic mechanical and thermal (DMT) analysis has become a widely used technique for determining the dynamic mechanical properties (dynamic modulus E^* storage modulus E' , loss modulus E'' and damping capacity $\tan \delta$) and interphase interaction of heterogeneous polymeric systems over a wide range of temperature.¹¹ The DMT analysis also helps to evaluate the viscoelastic behavior of polymer matrix in fiber reinforced composites at the glass transition region. The mechanical damping of composite material represents its capacity to reduce the dissipation of vibrational energy, which entirely depend upon the strength of fiber-matrix interfacial bonds. Many studies have been reported on the DMT properties of synthetic fibers reinforced thermoplastic composites filled with filler, impact modifier, compatibilizers, coupling agent etc. and also interpreted the fiber-matrix interfacial behavior by using DMA data.^{12–22} However, similar investigations on the polyolefin-elastomer blend based natural fiber composites have not received much attention.

Different polyolefins, e.g., HDPE, LDPE, polypropylene (PP) etc., as a homogeneous thermoplastic matrix were widely used for manufacturing of natural fiber reinforced composites.^{23–28} These composites

Correspondence to: A. Choudhury (arup@bitmesra.ac.in).

TABLE I
Physical, Chemical, and Mechanical Properties of Jute Fibers

Fiber	Diameter (μm)	Density (g cm^{-3})	Cellulose content (%)	Lignin content (%)	Tensile strength (MPa)	Tensile modulus (GPa)	Elongation (%)	Stiffness (GPa)	Micro-fibril angle (degree)
Jute	30	1.3–1.5	45–63	12–15	305	2.5–13	1.16	20–55	8

exhibited poor impact resistance particularly at low temperature, which considerably limits their application spectrum. However, the impact strength of the polyolefins was improved by blending with thermoplastic elastomer (e.g., EPDM).^{29,30} Some investigations on fiber reinforced PP-EPDM composites have been reported. Lopez-Manchado et al.^{31,32} have explored the reinforcing effects of different synthetic fibers on the crystallization kinetics, rheology, DMT and mechanical properties of PP-EPDM blends. The results showed that the fibers act as an effective reinforcing agent to PP-EPDM blends, but the reinforcing effect was more pronounced at low EPDM content in the blend ($\leq 25\%$). Similar phenomenon has also been observed by Arroyo et al.³³ in the case of short aramid fiber reinforced PP-EPDM composites. Arroyo and Bell³⁴ observed that the addition of aramid fibers to EPDM rich ($>50\%$) PP-EPDM blends sensible decreased the impact strength of the blend matrices, whereas the impact strength increased with increasing PP content ($>50\%$) in the blends. The different behavior of the aramid fibers depending upon the matrix type could be attributed to a better affinity of these fibers for PP-matrix. The mechanical performances of the natural flax fibers and conifer fibers reinforced PP-EPDM composites are analyzed by Biagiotti et al.³⁵ and Chuai et al.³⁶ respectively. Both types of fibers behave as an effective reinforcing agent to PP-EPDM systems. Siriwardena et al.³⁷ have studied the mechanical and DMT properties of white rice husk ash (WRHA) filled PP-EPDM blends before and after dynamic vulcanization. The incorporation of WRHA improved both the tensile and flexural modulus of polymer but lower the tensile strength, elongation at break, tear strength, and toughness of the matrix.

In the present investigation, the viability of maleic anhydride grafted polyethylene (MAPE) modified jute fiber reinforcement in LDPE-EPDM and HDPE-EPDM blends have been studied. The mechanical, thermal, and viscoelastic properties of treated jute fiber reinforced PE-EPDM composites were compared with untreated composites. The dependence on matrix composition, fiber loading, and MAPE concentration of various properties of these composites was also evaluated in this study. The fiber-matrix interface morphology was analyzed by SEM.

EXPERIMENTAL

Materials

The virgin LDPE (Indothene HD GC Exp 8A: MFI = $4.0 \text{ g } 10 \text{ min}^{-1}$ at 190°C , 2.16 kg load; Density = 0.922 g cm^{-3} at 23°C) and HDPE (M6805U: MFI = $0.5 \text{ g } 10 \text{ min}^{-1}$ at 190°C , 2.16 kg load; Density = 0.968 g cm^{-3} at 23°C) used for making the blends with EPDM were obtained from Indian Petrochemical and Haldia Petrochemical Ltd. India respectively. The EPR-g-MA (Exxelor 1803) containing 43 : 53 : 1.14 wt % ethylene/propylene/maleic anhydride was obtained from Exxon Chemical. The maleated EPR had a M_n of 40,000–50,000; melting points of 127°C and bra-bender torque of 9.76 Nm. Sodium hydroxide (NaOH) and acetic acid used for chemical treatment of the fibers were obtained from E. Merck India.

The short jute fibers (grade W-2, Chorchorus Capsularies) were collected from Indian Jute Industry Research Association (IJIRA), Kolkata. Table I presents the physical, chemical, and mechanical properties of the jute fibers.

Methods

Preparation of blends

The binary (80 : 20) LDPE-EPDM and (80 : 20) HDPE-EPDM blends were prepared by using Rheomex 254 single screw extruder fitted with a HAAKE Rheocord 9000 driving unit. The processing conditions followed for this extrusion are presented in Table II. The extruded mass was cooled by passing through water and subsequently pelletized. The pelletized mass was dried in a vacuum (0.657 atm) oven at 50°C for 12 h before subjecting it to any subsequent steps.

Chemical treatment of jute fibers

The short jute fibers (length $\sim 6.3 \text{ mm}$) were thoroughly washed by aqueous detergent solution to remove dirt followed by washing with distilled water and dried in vacuum oven at 50°C for 24 h.

Alkali treatment. The washed fibers were immersed in 5% aqueous NaOH solution for a period of 1 h at 30°C followed by washing with 0.1N acetic acid and distilled water. The alkali-treated fibers were then

TABLE II
Conditions Used in Rheomex 254 Single Screw Extrusion Process

Process	Temperature (°C)				Water bath	Screw speed (rpm)
	Zone 1	Zone 2	Zone 3	Zone 4		
Extrusion	200	220	240	250	30–35	60

dried in vacuum oven at 50°C for two days to obtain mercerized fibers.

Compatibilizer treatment. The mercerized jute fibers were immersed in different concentration (1, 2, and 3 wt %) of MAPE solutions (in toluene) at 60°C for 20 min to obtain compatibilizer coated fibers (treated jute fibers).

Composition fabrication

Composite mixtures were prepared by melt mixing the compatibilizer treated and untreated jute fibers with LDPE-EPDM and HDPE-EPDM blends in HAAKE Rheomix at 125°C, using roller blades and 60 cm³ mixing chamber of volumetric capacity. The process was carried out for a period of 10 min at an optimum speed of 50–60 rpm depending upon the

quantity (weight) of the fibers. Each batch contained various matrix compositions, fiber loading (10, 20, and 30 wt %) and MAPE concentrations (1, 2, and 3 wt %). The composite formulations are shown in Table III.

Each composite mixture was then homogenized in a two-roll mill (150E-400 Collins, Germany) at 130°C and compression molded using Delta Malikson 100TY pressman, to produce composite sheets (thickness 3 ± 0.2 mm). Test specimens were prepared from these sheets as per ASTM standard using Counter-cut copy milling machine 6490 (Ceast, Italy) with calibrated templates.

Characterizations

Mechanical properties. The rectangular bar specimens (dimension 80 × 12.7 × 3 mm³) of blend matrices

TABLE III
Formulations of LDPE-EPDM and HDPE-EPDM Blends Based Jute Fiber Composites

No	Sample abbreviation	LDPE (wt %)	HDPE (wt %)	EPDM (wt %)	Jute fiber (wt %)	MAPE (wt %)
LDPE-EPDM blend and LDPE-EPDM/jute fiber composites						
1	80LD-20EP	80	0	20	0	0
2	70LD-20EP-10J-0MAPE	70	0	20	10	0
3	70LD-20EP-10J-1MAPE	70	0	20	10	1
4	70LD-20EP-10J-2MAPE	70	0	20	10	2
5	70LD-20EP-10J-3MAPE	70	0	20	10	3
6	60LD-20EP-20J-0MAPE	60	0	20	20	0
7	60LD-20EP-20J-1MAPE	60	0	20	20	1
8	60LD-20EP-20J-2MAPE	60	0	20	20	2
9	60LD-20EP-20J-3MAPE	60	0	20	20	3
10	50LD-20EP-30J-0MAPE	50	0	20	30	0
11	50LD-20EP-30J-1MAPE	50	0	20	30	1
12	50LD-20EP-30J-2MAPE	50	0	20	30	2
13	50LD-20EP-30J-3MAPE	50	0	20	30	3
HDPE-EPDM blend and HDPE-EPDM/jute fiber composites						
14	80HD-20EP	0	80	20	0	0
15	70HD-20EP-10J-0MAPE	0	70	20	10	0
16	70HD-20EP-10J-1MAPE	0	70	20	10	1
17	70HD-20EP-10J-2MAPE	0	70	20	10	2
18	70HD-20EP-10J-3MAPE	0	70	20	10	3
19	60HD-20EP-20J-0MAPE	0	60	20	20	0
20	60HD-20EP-20J-1MAPE	0	60	20	20	1
21	60HD-20EP-20J-2MAPE	0	60	20	20	2
22	60HD-20EP-20J-3MAPE	0	60	20	20	3
23	50HD-20EP-30J-0MAPE	0	50	20	30	0
24	50HD-20EP-30J-1MAPE	0	50	20	30	1
25	50HD-20EP-30J-2MAPE	0	50	20	30	2
26	50HD-20EP-30J-3MAPE	0	50	20	30	3

LD, low density polyethylene (LDPE); HD, high density polyethylene (HDPE); EP, ethylene propylene diene copolymer (EPDM); J, jute fiber; MAPE, maleic anhydride grafted polyethylene.

and their jute fiber reinforced composites were subjected to flexural test (in accordance with ASTM D790) under three point bending in an Instron 3366 machine, using a crosshead speed of 2 mm min^{-1} and a span length of 50 mm. The Izod impact strength of notched samples (dimension $64 \times 12.7 \times 3 \text{ mm}^3$ with a V-notch depth of 2 mm and notch angle 45°) was measured in a Davenport Izod impact tester as per ASTM D256. The hardness was measured according to ASTM D2240 at room temperature (25°C) and expressed in Shore D hardness unit. Six measurements were performed for each sample, from which the standard deviation of the values was calculated.

Dynamic, mechanical, and thermal analysis. In the dynamic mechanical analysis, the specimens (dimension $35 \times 9 \times 2.45 \text{ mm}^3$) were clamped between strain gauges and subjected to small sinusoidal strain (static strain of 0.2% and dynamic strain of 0.1%) at the frequency of 0.1 Hz. The measurements were carried out at $35\text{--}150^\circ\text{C}$ temperature range with a rate of heating 3°C min^{-1} . The machine used in this measurement was 2980 DMA V1.7B.

Differential scanning calorimetric analysis. The thermal behavior of polymer matrix and composite samples was measured by DSC analysis in both N_2 and O_2 atmosphere, using TA 10Q-DSC analyzer. The heating scan was performed from 30 to 300°C at a rate of $10^\circ\text{C min}^{-1}$. The degree of crystallinity (X_{cr}) was determined according to the relation: $X_{\text{cr}} = 100 \times (\Delta H / \Delta H_0)$, where ΔH is the enthalpy of fusion of the polyethylene (PE) component as calculated from the DSC analysis, and ΔH_0 is the enthalpy of fusion of the 100% crystalline PE. In all cases the heat of fusion of 290 J g^{-1} has been taken for 100% crystalline PE.³⁸

Scanning electron microscopic analysis. To study the morphological features of fiber-matrix interface in the MAPE treated and untreated composite samples, the flexural test samples were fractured after 15–20 min of freezing in liquid nitrogen. The fractured surfaces were sputtered with gold and analyzed with a JEOL JSM 5000 scanning electron microscopy (Peabody, MA).

RESULTS AND DISCUSSION

Mechanical properties

The most conventional chemical treatment for surface modification of jute fiber is mercerization (alkali treatment). Further the jute fiber surface was coated with MAPE to make the fibers more hydrophobic and to improve interfacial adhesion between fiber and matrix (PE-EPDM blends) via formation of ester linkage with $-\text{OH}$ groups of jute cellulose fiber and cyclic anhydride groups of MAPE. FTIR spectra of MAPE-coated and uncoated jute fibers are reported

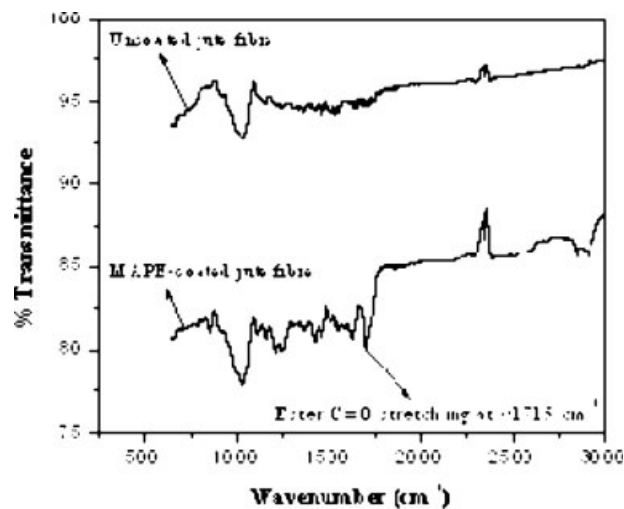


Figure 1 FTIR spectra of MAPE-coated and uncoated jute fibers.

in Figure 1. The spectra of MAPE-coated jute fibers, as compared to uncoated jute, show a marked absorption peak in the carbonyl region ($\sim 1715 \text{ cm}^{-1}$), which are associated with the ester group formed between fiber and MAPE. As a result, the composites reinforced with treated fibers showed better mechanical properties (flexural strength, flexural modulus, impact strength, and hardness). The properties of matrix and fiber are very important aspects in achieving good mechanical properties of the composites. The melt strength and processability are the most sensitive parameter to polymer matrix, whereas the modulus is dependent on fiber properties.³⁹ The variation of flexural properties (strength and modulus) of PE-EPDM-based jute fiber composites as a function of fiber loading and MAPE dose are shown in Figure 2(a,b) respectively. As observed in Figure 2(a), the flexural strength and modulus were sharply increased with increasing fiber loading for both LDPE-EPDM/jute fiber and HDPE-EPDM/jute fiber composites (at 3% MAPE concentration). The increase in mechanical strength with fiber loading is primarily attributed to reinforcing effect imparted by the fibers, which allowed a uniform stress distribution from polymer matrix to dispersed fiber phase.⁴⁰ Similarly, the enhancement of modulus at higher fiber loading is due to the fact that the fibers act as points of mechanical restraint in the system and consequently restrict the mobility of the polymer chains during mechanical deformation. It can also be seen from Figure 2(a) that both flexural strength and modulus are recorded higher for HDPE-EPDM/jute fiber composites compared to LDPE-EPDM/jute fiber composites at 3% MAPE concentration, which is due to less plasticizing effect of EPDM rubber in higher crystallinity HDPE phase compared to that in less crystalline LDPE system.

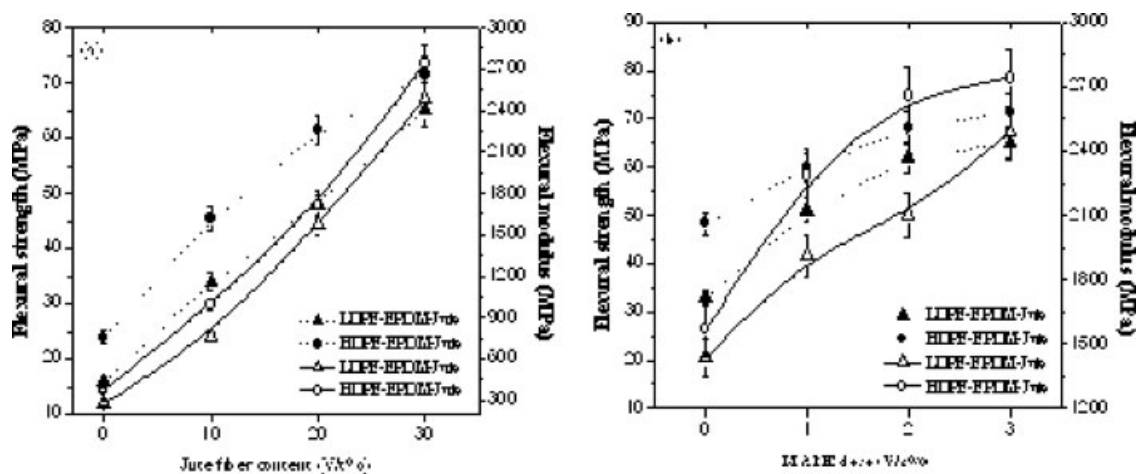


Figure 2 Effect of (a) fiber loading (at 3% MAPE dose) and (b) MAPE dose (with 30% fiber content) on flexural strength (dot line) and flexural modulus (solid line) of jute fiber reinforced LDPE-EPDM and HDPE-EPDM composites.

The plasticizing effect of EPDM (amorphous in nature) is much higher in LDPE-EPDM matrix because of its better miscibility with LDPE, which leads to increase the chain mobility and thus reduce the modulus of the LDPE-EPDM/jute composites compared to HDPE-EPDM/jute composites. As shown in Figure 2(b), all the treated PE-EPDM/jute fiber composites exhibited superior flexural strength and modulus compared to untreated composites at 30 wt % fiber loading. However, the flexural properties of the treated composites were significantly increased with increasing MAPE concentration [Fig. 2(b)]. This phenomenon indicates that the addition of compatibilizer (MAPE) improves the interfacial adhesion between fiber and matrix in the composites.

The effect of fiber loading and compatibilizer dose on notched impact strength and hardness of the different formulated PE-EPDM-based jute fiber composites are graphically presented in Figure 3(a,b). A pro-

nounced increase in impact strength of the composites was observed as the fiber loading increased from 0 to 30 wt %, shown in Figure 3(a). Similar results for aramid fibers reinforced PE-EPDM composites are also observed by earlier author.³⁴ Further, the impact strength of LDPE-EPDM/jute composites was recorded higher than that of HDPE-EPDM/jute composites at 3% MAPE concentration. The results indicate that the EPDM rubber act as better impact modifier for the LDPE-EPDM matrix rather HDPE-EPDM system, which is due to higher miscibility between LDPE and EPDM components. Therefore, LDPE-EPDM/jute fiber composites have better energy absorbing capacity compared to HDPE-EPDM/jute composites. The variation of hardness follows the same trend as observed for flexural properties of the composites as a function of fiber loading [Fig. 3(a)]. As shown in Figure 3(b), both impact strength and hardness of the composites were considerably enhanced with

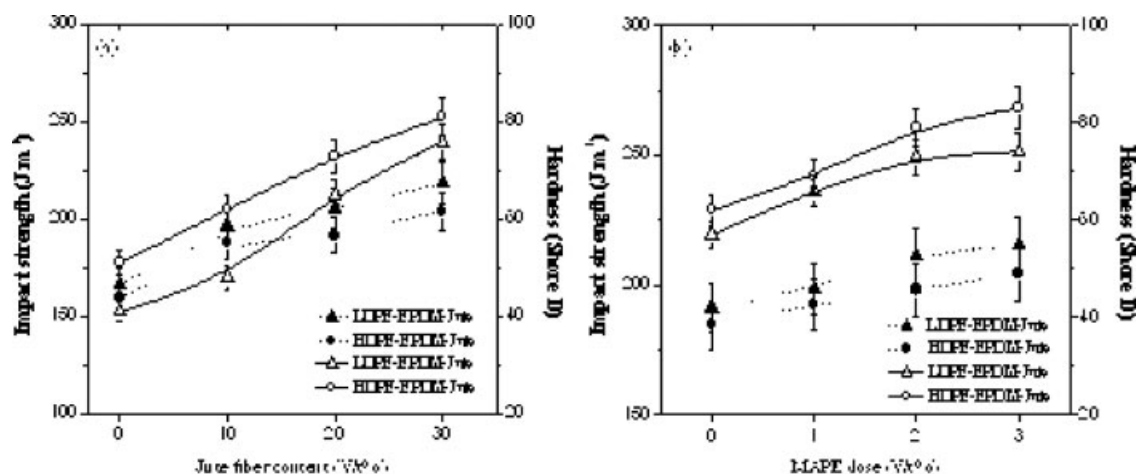


Figure 3 Effect of (a) fiber loading (at 3% MAPE dose) and (b) MAPE dose (with 30% fiber content) on impact strength (dot line) and hardness (solid line) of jute fiber reinforced LDPE-EPDM and HDPE-EPDM composites.

TABLE IV
The Values of Slopes Calculated From Mechanical Properties Versus Fiber Loading/MAPE Dose Plots in Figure 1 and 2

Composites	Slopes of mechanical properties versus fiber loading plots				Slopes of mechanical properties vs. MAPE dose plots			
	Flexural strength	Flexural modulus	Impact strength	Hardness	Flexural strength	Flexural modulus	Impact strength	Hardness
LDPE-EPDM/jute	1.52	70.17	1.53	1.13	10.7	182.3	8.90	6.7
HDPE-EPDM/jute	1.42	66.08	1.22	0.96	7.77	103.5	6.49	7.3

increasing MAPE dose from 0 to 2% followed by marginal increment to 3% MAPE concentration. The addition of compatibilizer improves the fiber-matrix interfacial adhesion and thus, increases the energy absorbing capacity of the composites.

However, the rate of improvement in mechanical properties of the LDPE-EPDM/jute and HDPE-EPDM/jute composites as a function of fiber loading and MAPE dose was assessed by determining the slope of the mechanical properties versus fiber loading/MAPE dose plots, shown in [Figs. 2(a,b) and 3(a,b)]. The slopes of the different plots in Figure 2(a,b) and 3(a,b) are presented in Table IV. As observed in Table IV, the magnitude of the slopes for LDPE-EPDM/jute composites are recorded higher compared to those of HDPE-EPDM/jute composites. It indicates that rate of improvement in mechanical properties of the LDPE-EPDM blend with incorporation of fibers and MAPE is more superior to that of HDPE-EPDM blend, which is due to higher miscibility between LDPE and EPDM components.

Dynamic mechanical properties

The dynamic mechanical properties of composites are significantly dependent upon the amount of

fiber,^{41,42} the presence of additives-like compatibilizer, filler, and impact modifier,⁴³ fiber orientation,⁴⁴ and mode of testing. In practice, polymer materials exhibit more than one relaxation regions or so-called transition over a wide range of temperature during dynamic thermomechanical analysis. The variations of dynamic mechanical properties (storage modulus, loss modulus, and $\tan \delta$) with temperature for different formulated PE-EPDM blends and PE-EPDM-based jute fiber composites are graphically presented in Figures 4–9. It can be seen from Figure 4(a,b) that there was a notable increase in the storage modulus (E') of LDPE-EPDM and HDPE-EPDM blends with incorporation of jute fibers (at 3% MAPE concentration). This behavior is due to the increase in stiffness of the blend matrices as a result of fiber reinforcement that allowed greater stress transfer from matrix to fiber at the interface. It also appeared that the E' values of HDPE-EPDM/jute composites are recorded higher than those observed for LDPE-EPDM/jute composites, which might be due to the stiffer nature of highly crystalline HDPE component. Although, the rate of fall of storage modulus (dE'/dT) values with temperature for the HDPE-EPDM/jute fiber composites is higher than that of LDPE-EPDM/jute fiber composites, shown in Figure 4(a,b). This could

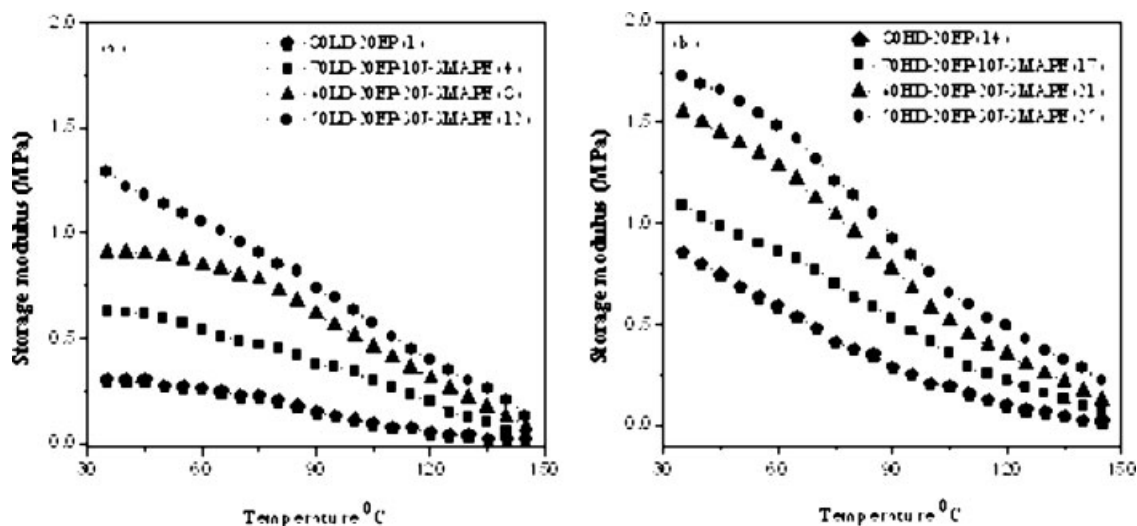


Figure 4 Variation of storage modulus with temperature of (a) LDPE(LD)-EPDM(EP) blend and jute fiber (J) composites; and (b) HDPE(HD)-EPDM blend and jute fiber composites, at 3% MAPE concentration.

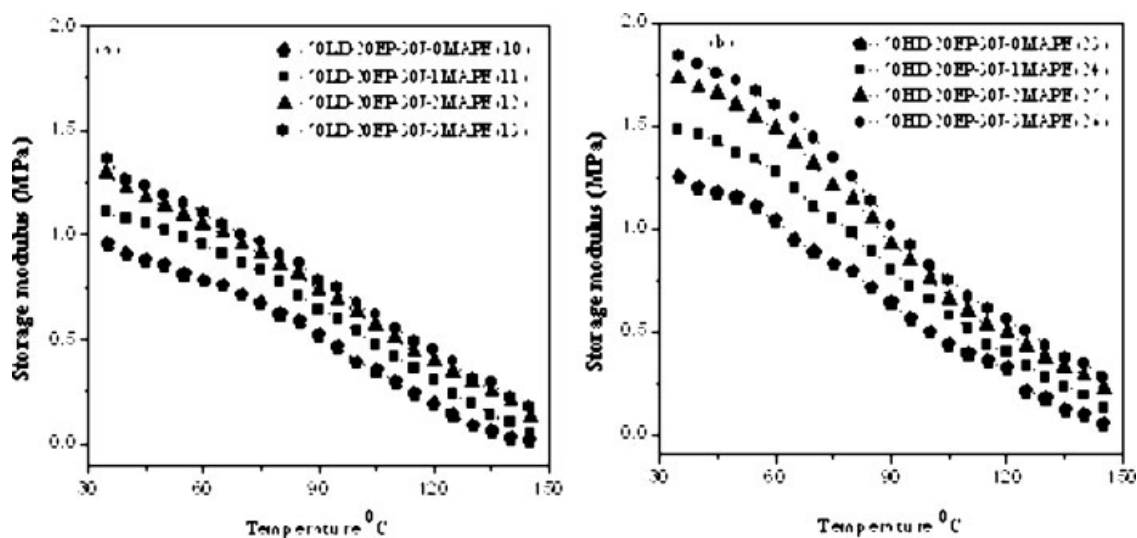


Figure 5 Effect of MAPE dose on storage modulus of (a) LDPE(LD)-EPDM(EP); and (b) HDPE(HD)-EPDM blends based jute fiber (J) composites, at 30% fiber content.

be attributed to greater defect concentration (total amount of defects in the fibers as well as fiber-matrix interface) in the HDPE-EPDM/jute fiber composites, because the presence of discontinuous EPDM phase in HDPE-EPDM matrix incorporated maximum defects during melt mixing with jute fibers. The effect of compatibilizer treatment on the storage modulus of LDPE-EPDM and HDPE-EPDM blends based jute composites are presented in Figure 5(a,b). It is evident from these figures that the treated composites (formulation no 11–13 and 24–26) exhibited higher E' values in comparison to untreated composites (formulation no 10 and 23) at same fiber loading (30 wt %). Further, the E' values increased with increasing compatibilizer concentration from 1 to

3%. The 50%LDPE-20%EPDM/30%jute fiber composites (formulation no 10–13) showed $\sim 65.8\%$ increase in flexural modulus and $\sim 35.4\%$ in storage modulus with 3% MAPE treatment. On the other hand, $\sim 75.7\%$ increase in flexural modulus and $\sim 45.7\%$ in storage modulus were achieved for 50%HDPE-20%EPDM/30%jute fiber composites (formulation no 23–26) by same treatment. This behavior is primarily attributed to improvement of interfacial adhesion between treated fibers and matrix.

Figure 6(a,b) and 7(a,b) show the variation of loss modulus (E'') with temperature for LDPE-EPDM/jute and HDPE-EPDM/jute composites containing different jute fiber content (10, 20, and 30 wt %) and MAPE concentration (1, 2, and 3 wt %) respectively.

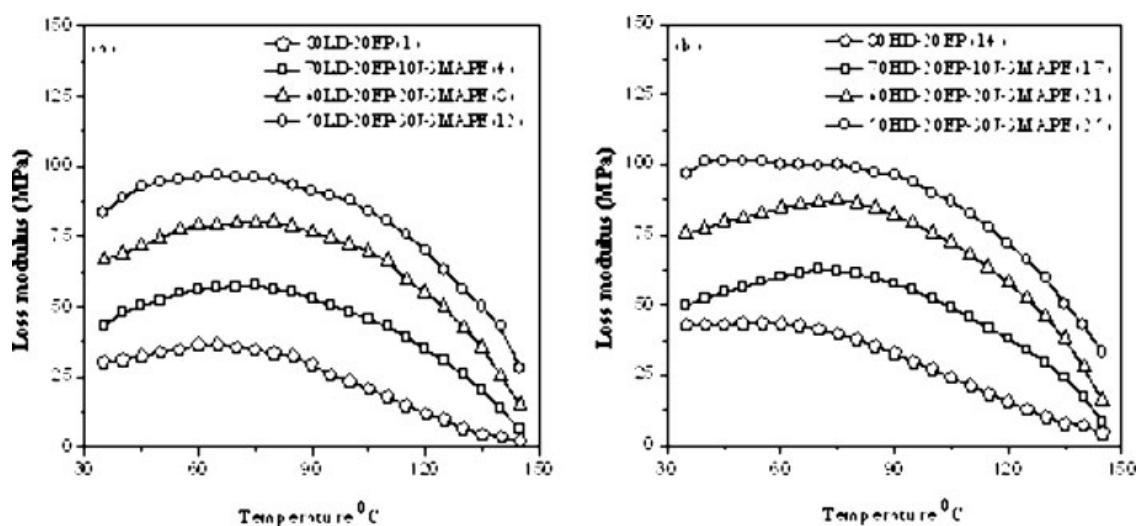


Figure 6 Variation of loss modulus with temperature of (a) LDPE(LD)-EPDM(EP) blend and jute fiber (J) composites; and (b) HDPE(HD)-EPDM blend and jute fiber composites, at 3% MAPE concentration.

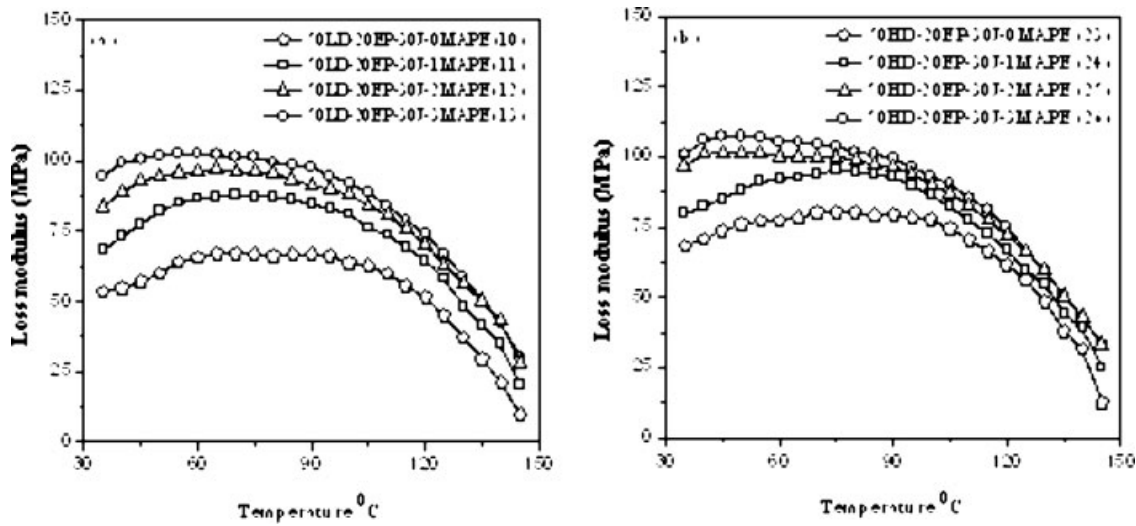


Figure 7 Effect of MAPE dose on loss modulus of (a) LDPE(LD)-EPDM(EP); and (b) HDPE(HD)-EPDM blends based jute fiber (J) composites, at 30% fiber content.

The loss modulus curves show a α -relaxation peak between 70 and 120°C. The α -relaxation associated with the chain segment mobility in the crystalline phases, which might be due to reorientation of defect areas in the crystal. As appeared in the Figures 6(a,b) and 7(a,b), the α -relaxation peak of polymer matrix (LDPE-EPDM and HDPE-EPDM blends) was shifted toward higher temperature region with the incorporation of jute fibers and MAPE. The corresponding loss modulus values at this temperature increased with increasing fiber loading [Fig. 6(a,b)], which is related to the reduction of flexibility of the composite materials by introducing constraints on the segmental mobility of polymer chains in presence of jute fibers.³² The broadening of transition peak was increased with increase in fiber loading

[Fig. 6(a,b)], which is due to the increase in energy absorption (less viscous dissipation) caused by fiber reinforcement.

The ratio of loss modulus to storage modulus (E''/E') is measured as the mechanical loss factor or $\tan \delta$. The variation of $\tan \delta$ as a function of temperature for different formulated matrix and composite samples is shown in Figures 8(a,b) and 9(a,b). As shown in Figure 8(a,b), the $\tan \delta$, which is corresponding to the damping properties of the material, is found to be decreased with increase in the fiber content at 3% MAPE concentration. The increase in fiber loading also reduced the peak height of $\tan \delta$. The reason could be attributed to the restriction of the chain mobility by fiber reinforcement, which raised the storage modulus values and reduced the viscoelastic lag

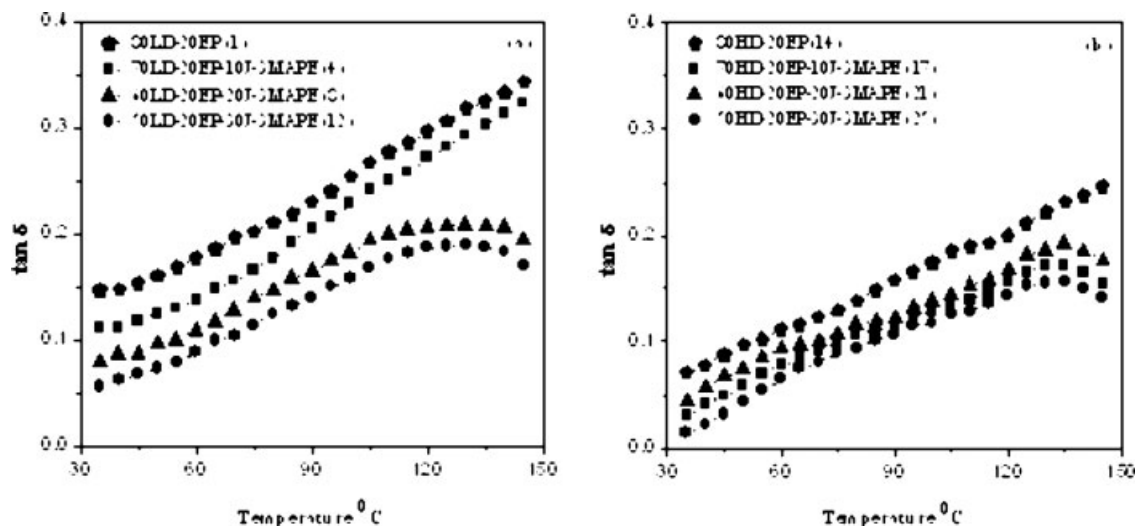


Figure 8 Variation of $\tan \delta$ with temperature of (a) LDPE(LD)-EPDM(EP) blend and jute fiber (J) composites; and (b) HDPE(HD)-EPDM blend and jute fiber composites, at 3% MAPE concentration.

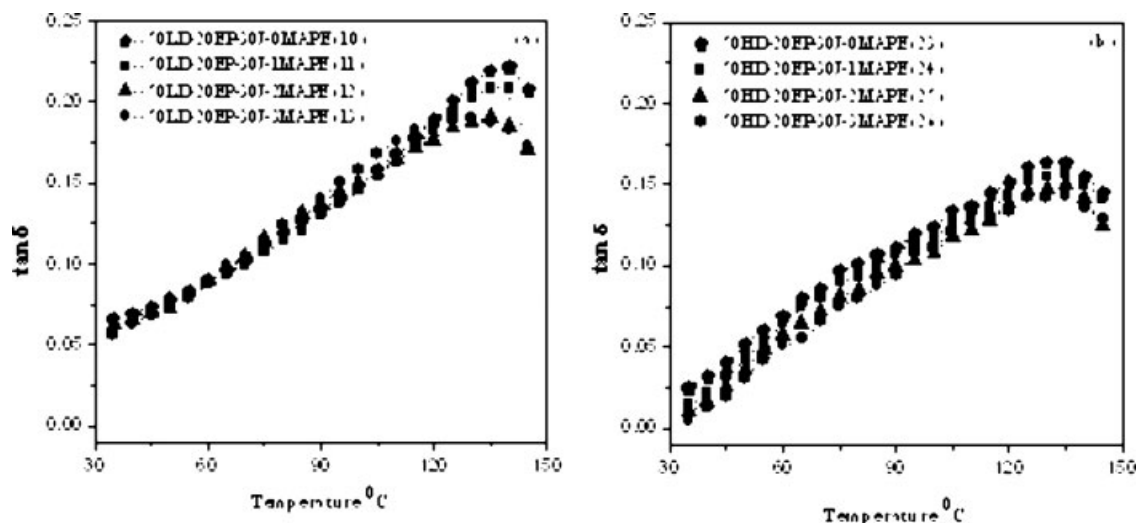


Figure 9 Effect of MAPE dose on $\tan \delta$ of (a) LDPE(LD)-EPDM(EP); and (b) HDPE(HD)-EPDM blends based jute fiber (J) composites, at 30% fiber content.

between the stress and the strain and hence, decreased the $\tan \delta$ values with increase in the fiber loading.⁴⁵ The $\tan \delta$ values of untreated composites (formulation no 10 and 23) are observed to be higher than that of the treated composites (formulation no 11–13 and 24–26) and further, the $\tan \delta$ decreased with increasing the MAPE concentration [Fig. 9(a,b)]. This results could be interpreted that for untreated composites, the poor interfacial bonding between fibers and matrix tend to dissipate more energy, showing high magnitude of $\tan \delta$ (damping peak) in comparison to the treated composites having strongly bonded interface.⁴⁶

Thermal properties

To characterize the thermal behavior of LDPE-EPDM and HDPE-EPDM blends before and after jute fiber reinforcement, DSC analysis was carried out in both N_2 and O_2 atmospheres. In the DSC measurement in N_2 atmosphere, one broad melting peak at $\sim 112^\circ\text{C}$ for LDPE-EPDM blends/jute composites and same at $\sim 126^\circ\text{C}$ for HDPE-EPDM blends/jute composites were found. The theoretical crystalline melting temperature (T_m) for LDPE is $\sim 110^\circ\text{C}$ and that for HDPE is $\sim 128^\circ\text{C}$. The details of this analysis are presented in Table V. As appeared in Table V, the T_m , percent crystallinity and oxidation temperature (T_{ox}) of the polymer matrix was significantly influenced by the incorporation of fibers and MAPE. The T_m of LDPE and HDPE components were recorded lower for treated composites compared to the untreated composites and, follow decreasing trend with increasing fiber loading and MAPE dose. The lowering in melting temperatures with incorporation of compatibilizer indicates that the crystallization process occur more

rapidly and those crystal formed are smaller, which probably due to nucleation effect imparted by the compatibilizer for the PE. The addition of fibers was significantly reduced the percent crystallinity of the polymer matrix, shown in Table V, which is attributed to the reduction in structural regularity and close packing ability of the polymer chains in presence of fibers, and hence decreases the polymer crystallinity. However, the polymers with high thermal stability are always challenging criteria to every industry for enhancement of durability of the products. As observed in Table V, both onset and peak oxidation temperatures of the PE-EPDM blends significantly enhanced with fiber loading. It indicates that the oxidative stability of polymer matrix was remarkable increased by fiber reinforcement, which is due to heat deflection property of fibers. It can also be seen from Table V that the T_{ox} values were recorded higher for the MAPE treated composites compared to untreated composites. Nearly 6°C increase in T_{ox} was noticed with 3% MAPE treatment. It indicates that oxidative stability of the PE-EPDM-based jute fiber composites could enhance by addition of optimum concentrations of fibers and compatibilizer.

Morphological investigation

Morphological studies were carried out to investigate the fiber surface morphology, fiber pull out and fiber-polymer interface in the untreated and treated composites by scanning electron microscopy (SEM). The SEM photomicrographs of the cryogenic fractured surfaces of treated and untreated LDPE-EPDM/jute composites at 30% fiber loading and those of HDPE-EPDM/jute composites are illustrated in Figures 10(a,b) and 11(a,b) respectively. In

TABLE V
DSC Data Obtained for Polymer Matrix and Jute Fiber Reinforced Composites

Sample formulations	DSC in N ₂		DSC in O ₂	
	^a T _m (°C)	^b X _{cr}	Onset ^c T _{ox} (°C)	Peak ^c T _{ox} (°C)
80LD-20EP (1)	116.2	30.6	190.4	208
70LD-20EP-10J-0MAPE (2)	114.2	27.6	191.5	210
70LD-20EP-10J-1MAPE (3)	113.6	27.9	192.6	211
70LD-20EP-10J-2MAPE (4)	113.8	28.6	193.0	213
70LD-20EP-10J-3MAPE (5)	112.4	28.4	194.7	214
60LD-20EP-20J-0MAPE (6)	113.7	26.1	193.6	212
60LD-20EP-20J-1MAPE (7)	112.4	27.3	194.5	213
60LD-20EP-20J-2MAPE (8)	113.1	27.6	195.2	215
60LD-20EP-20J-3MAPE (9)	112.1	27.9	197.8	216
50LD-20EP-30J-0MAPE (10)	111.3	24.2	195.1	214
50LD-20EP-30J-1MAPE (11)	109.4	24.7	197.4	215
50LD-20EP-30J-2MAPE (12)	110.0	25.5	197.3	217
50LD-20EP-30J-3MAPE (13)	107.5	25.0	199.8	219
80HD-20EP (14)	128.3	38.7	195.7	213
70HD-20EP-10J-0MAPE (15)	126.5	35.4	197.4	214
70HD-20EP-10J-1MAPE (16)	126.1	35.7	197.8	215
70HD-20EP-10J-2MAPE (17)	125.0	35.9	199.3	216
70HD-20EP-10J-3MAPE (18)	126.1	36.6	201.7	219
60HD-20EP-20J-0MAPE (19)	125.7	34.1	199.1	216
60HD-20EP-20J-1MAPE (20)	124.3	34.5	204.8	218
60HD-20EP-20J-2MAPE (21)	123.5	34.4	204.0	219
60HD-20EP-20J-3MAPE (22)	123.0	35.2	208.1	221
50HD-20EP-30J-0MAPE (23)	125.3	33.0	204.6	220
50HD-20EP-30J-1MAPE (24)	124.6	33.4	206.4	222
50HD-20EP-30J-2MAPE (25)	123.4	33.4	207.8	224
50HD-20EP-30J-3MAPE (26)	122.8	33.8	209.2	226

^a Crystalline melting temperature.

^b Percent crystallinity.

^c Oxidation temperature.

the case of untreated composites [Figs. 10(b) and 11(b)], the fibers appeared to be free from the polymer matrix and a large number of holes or voids resulting from extensive fiber pull out were observed. This indicates poor interfacial adhesion and inadequate wetting of the untreated fibers within the nonpolar PE-EPDM matrix, which is due

to large difference in surface energies between the fibers and the matrix. For treated composites, considerably less number of fiber pull outs (less number of holes) and fiber broken ends embedded in the polymer matrix were observed, shown in Figures 10(a) and 11(a). It is clearly indicating that the incorporation of compatibilizer (MAPE) effectively developed

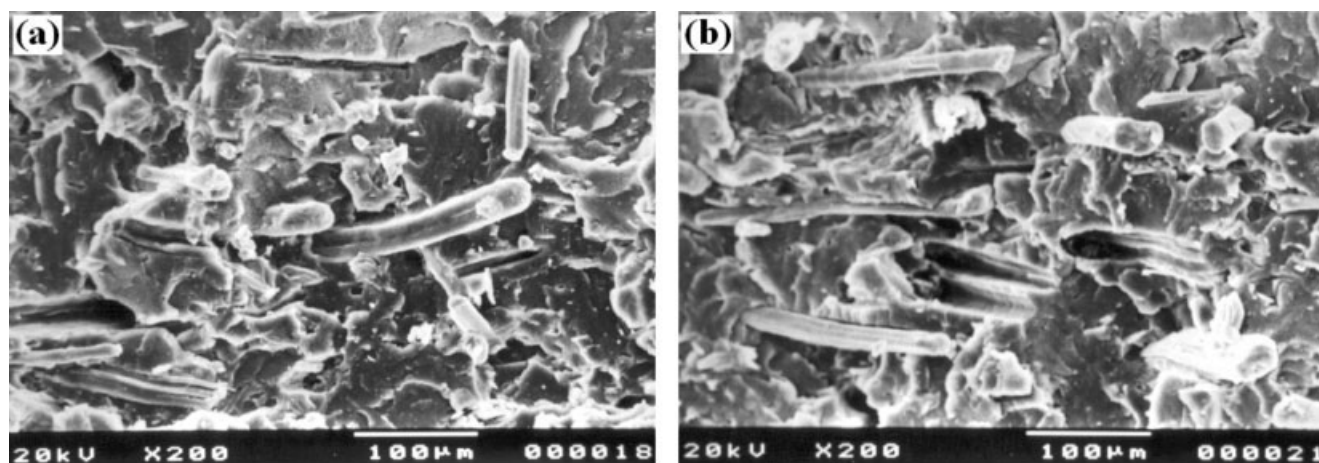


Figure 10 SEM photomicrographs of (a) treated (3% MAPE); and (b) untreated LDPE-EPDM-based jute fiber composites at 30% fiber loading.

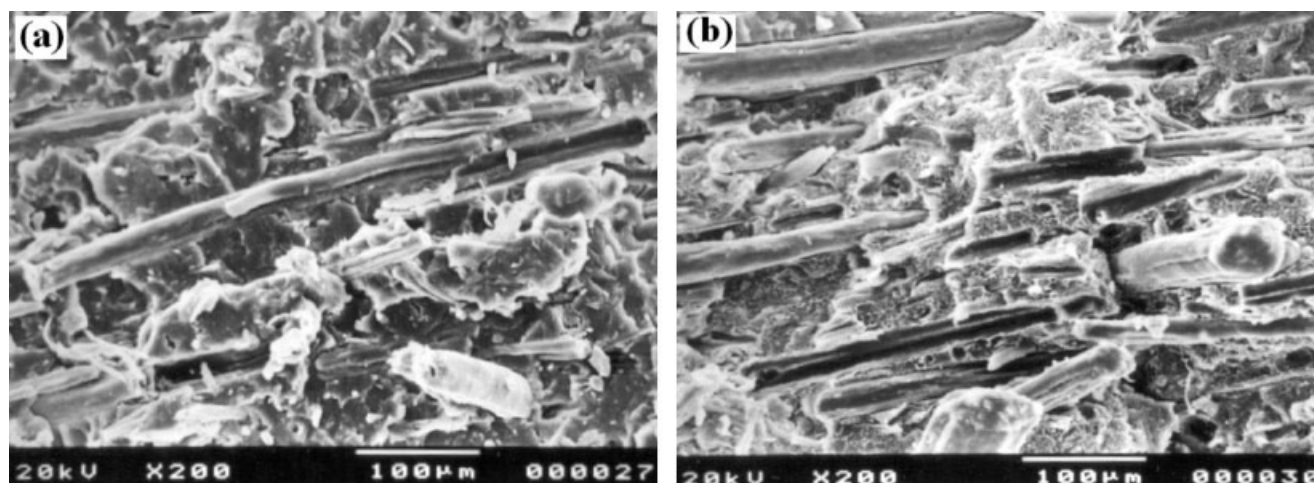


Figure 11 SEM photomicrographs of (a) treated (3% MAPE); and (b) untreated HDPE-EPDM-based jute fiber composites at 30% fiber loading.

strong interfacial bonding between fibers and matrix in the composites, which is reflected on their mechanical performances.

CONCLUSIONS

The mechanical, thermal, and dynamic mechanical properties of (80:20) LDPE-EPDM and HDPE-EPDM blends based jute fiber composites have been investigated. All the flexural strength, flexural modulus, impact strength, and hardness of the composites increased with increase in both fiber loading (at 3% MAPE concentration) and MAPE dose (at 30 wt % fiber content). The maximum values of flexural properties and hardness were achieved for HDPE-EPDM/jute fiber composites, whereas LDPE-EPDM/jute fiber composites showed higher impact strength. However, the rate of improvement in mechanical properties of the LDPE-EPDM blend with incorporation of fibers and MAPE is found to be higher than that of the HDPE-EPDM system. The difference in mechanical properties between the untreated and the treated composites could be corroborated with morphological evidences and DMA studies. Storage modulus versus temperature plots showed an increase in stiffness of the PE-EPDM matrix as result of jute fiber reinforcement. The damping peaks ($\tan \delta$) of treated composites showed lower magnitude as compared to untreated composites and further, the $\tan \delta$ values decreased with increase in both fiber content and MAPE concentration. The thermo-oxidative stability of polymer matrix was significantly increased by fiber reinforcement, however, the treated composites exhibited better stability compared to untreated composites. Nearly 6°C increase in oxidation temperature was noticed with

3% MAPE treatment. On the basis of above studies, it can be concluded that an optimal concentration of jute fibers and MAPE could effectively reinforce the PE-EPDM blends and enable to achieve satisfactory properties of the composites for various engineering applications.

References

- Pervaiz, M.; Sain, M. M. *Macromol Mater Eng* 2003, 288, 553.
- C.C.M. Ma. *First Asian Australasian Conference on Composite Materials (ACCM-1)*; Osaka, Japan 1998, p 205.
- Hashmi, S. A. R.; Kitano, T.; Chand, N. *Polym Compos* 2003, 24, 149.
- Karger-Kocsis, J. *Polypropylene: Structure, Blends and Composites*; London: Chapman and Hall, 1995; Vol. 3.
- Bledzki, A. K.; Gassan, J. *Prog Polym Sci* 1999, 24, 221.
- Mohanty, A. K.; Misra, M.; Hinrichsen, G. *Macromol Mater Eng* 2000, 276/277, 1.
- Brahmakumar, M.; Pavithran, C.; Pillai, R. M. *Compos Sci Technol* 2005, 65, 563.
- Park, J. M.; Quang, S. T.; Hwang, B. S.; Lawrence De Vries, K. *Compos Sci Technol* 2006, 66, 2686.
- Arzondo, L. M.; Perez, C. J.; Carella, J. M. *Polym Eng Sci* 2005, 45, 613.
- Rigoberto, B.; Mario, J. Q.; Mohanty, A. K.; Mehta, G.; Lawrence, T. D.; Misra, M. *Compos A: Appl Sci Manuf* 2005, 36, 581.
- Ray, D.; Sarkar, B. K.; Das, S.; Rana, A. K. *Compos Sci Technol* 2002, 62, 911.
- Botev, M.; Betchev, H.; Bikiaris, D.; Panayiotou, C. *J Appl Polym Sci* 1999, 74, 523.
- Sohn, M. S.; Kim, K. S.; Hong, S. H.; Kim, J. K. *J Appl Polym Sci* 2003, 87, 1595.
- Beaudoin, O.; Bergeret, A.; Quantin, J. C.; Crespy, A. *Polym Compos* 2002, 23, 87.
- Vajrasthira, C.; Amornsakchai, T.; Limcharoen, B. *J Appl Polym Sci* 2003, 87, 1059.
- Verghese, K. N. E.; Jensen, R. E.; Lesko, J. J.; Ward, T. C. *Polymer* 2001, 42, 1633.
- Sengupta, P. K.; Mukhopadhyay, D. *J Appl Polym Sci* 2003, 51, 831.

18. Ratna, D.; Chongdar, T. K.; Chakraborty, B. C. *Polym Int* 2000, 49, 815.
19. Mohd Ishak, Z. A.; Berry, J. P. *Polym Compos* 2004, 15, 223.
20. Goertzen, W. K.; Kessler, M. R. *Compos B: Eng* 2007, 38, 1.
21. Larena, A.; Jiménez de Ochoa, S.; Domínguez, F. *Polym Degrad Stab* 2006, 91, 940.
22. Wilson, T. W.; Fornes, R. E.; Gilbert, R. D.; Memory, J. D. *J Polym Sci B: Polym Phys* 2003, 26, 2029.
23. Dányádi, L.; Renner, K.; Szabó, Z.; Nagy, G.; Móczó, J.; Pukánszky, B. *Polym Adv Technol* 2006, 17, 967.
24. Mohanty, S.; Verma, S. K.; Tripathy, S. S.; Nayak, S. K. *J Reinf Plast Compos* 2004, 23, 625.
25. Mohanty, S.; Verma, S.K.; Nayak, S.K. *Compos Sci Technol* 2006, 66, 538.
26. Mohanty, S.; Verma, S. K.; Nayak, S. K.; Tripathy, S. S. *J Appl Polym Sci* 2004, 94, 1336.
27. Baroulaki, I.; Mergos, J. A.; Pappa, G.; Tarantili, P. A.; Economides, D.; Magoulas, K.; Dervos, C. T. *Polym Adv Technol* 2006, 17, 954.
28. Li, T.; Yan, N. *Compos A: Appl Sci Manufact* 2007, 38, 1.
29. Van der Wal, A.; Gaymans, R. J. *Polymer* 1999, 40, 6067.
30. Van der Wal, A.; Mulder, J. J.; Oderkerk, J.; Gaymans, R. J. *Polymer* 1998, 39, 6781.
31. López Manchado, M. A.; Torre, L.; Kenny, J. M. *J Appl Polym Sci* 2001, 81, 1063.
32. Lopez-Manchado, M. A.; Biagiotti, J.; Kenny, J. M. *Polym Compos* 2002, 23, 779.
33. Arroyo, M.; Zitzumbo, R.; Avalos, F. *Polymer* 2000, 41, 6351.
34. Arroyo, M.; Bell, M. *J Appl Polym Sci* 2002, 83, 2474.
35. Biagiotti, J.; López-manchado, M. A.; Arroyo, M.; Kenny, J. M. *Polym Eng Sci* 2004, 43, 1031.
36. Chuai, C.; Almdal, K.; Poulsen, L.; Plackett, D. *J Appl Polym Sci* 2001, 80, 2833.
37. Siriwardena, S.; Ismail, H.; Ishiaku, U. S.; Perera, M. C. S. *J Appl Polym Sci* 2002, 85, 438.
38. Utracki, L. A.; *Polymer Alloys and Blends*; Hanser-Munich: New York, 1989.
39. Hull, D. *An Introduction to Composite Materials*, 2nd ed.; Cambridge University Press: Cambridge, 1996; p 326.
40. Colom, X.; Carrasco, F.; Pages, P.; Canavate, J. *Compos Sci Technol* 2003, 63, 161.
41. Tasi, S. W.; Halpin, H. T. *Introduction to Composites Materials*; Technomic: Westport, CT, 1980.
42. Adams, R. D.; Short, D. F. *J Phys D: Appl Phys* 1973, 6, 1032.
43. Kolarik, F.; Lednický, F.; Pukánszky, B. *Compos Mater* 1987, 6, 452.
44. Adams, R. D.; Doner, D. R. *J Compos Mater* 1967, 1, 4.
45. Ghose, P.; Bose, N. R.; Mitra, B. C.; Das, S. *J Appl Polym Sci* 1997, 62, 2467.
46. Ashida, M.; Noguchi, T. *J. Appl Polym Sci* 1984, 29, 661.